Conversion of Amyloid Fibrils of Cytochrome c to Mature Nanorods through a Honeycomb Morphology

ARTICLE *in* LANGMUIR · OCTOBER 2014

Impact Factor: 4.46 · DOI: 10.1021/la5029993 · Source: PubMed

4 AUTHORS, INCLUDING:

Shubhasis Haldar
University of California
11 PUBLICATIONS **101** CITATIONS
SEE PROFILE

Krishnananda Chattopadhyay
Indian Institute of Chemical Biology
40 PUBLICATIONS **913** CITATIONS
SEE PROFILE

Langmuir

Article

pubs.acs.org/Langmuir

Conversion of Amyloid Fibrils of Cytochrome c to Mature Nanorods through a Honeycomb Morphology

Shubhasis Haldar, Pallabi Sil, Muruganandan Thangamuniyandi, and Krishnananda Chattopadhyay*

Protein Folding and Dynamics Laboratory, Structural Biology and Bioinformatics Division, CSIR-Indian Institute of Chemical Biology, 4 Raja S. C. Mullick Road, Kolkata 700032, India

Supporting Information

ABSTRACT: Amyloid species with various morphologies have been found for different proteins and disease systems. In this article, we aim to ask if these morphologies are unique to a particular protein or if they convert from one to another. Using a heme protein containing iron as the transition-metal activator of aggregation and a negatively charged surfactant, partial unfolding of the protein and its aggregation have been induced. In the pathway of aggregation, we have observed the formation of several morphological structures of a single protein, which were visualized directly using atomic force microscopy (AFM). These structures have been found to appear and disappear with time, and their formation could be monitored under normal buffer conditions and at room temperature without requiring any sophisticated chemical or biological methodologies. In addition, we have observed the formation of honeycomb-shaped morphology, which may serve as an intermediate. These amyloid-based nanostructures may have the potential to be explored in therapeutics delivery and other biomedical applications.

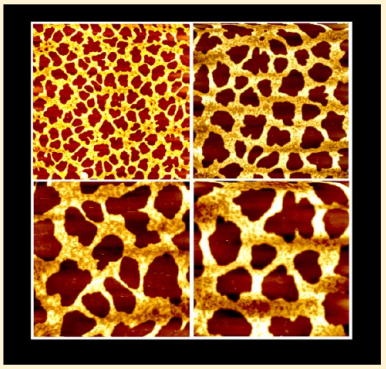

INTRODUCTION

The generation of amyloid structures is often believed to be a common feature of a variety of human diseases, including Alzheimer's disease, Parkinson's disease, type 2 diabetes, and prion diseases. Amyloid structures are not always harmful. Various living organisms form amyloid fibrils using their endogenous proteins to carry out normal physiological functions. From the biotechnology perspective, amyloids are being used in various fields, including molecular electronics, drug delivery, and tissue engineering.[1]

The structure, dynamics, and mechanism of amyloid formation have been thoroughly investigated in the current literature.[2−5] However, structural plasticity in the late stages of amyloid formation remains an interesting problem. Amyloid fibrils have been shown to exist in different morphological structures, depending on the protein of interest and/or the implicated disease conditions.[6−9] For example, amyloid fibrils with a ribbon width of 10 nm have been observed for α-synuclein, the major player in Parkinson's disease, whereas a giant multistranded twisted structure (width of 173 nm) has been observed for both lysozyme and β-lactoglobulin.[6] Amyloid pore structures of different morphology have been observed in α-synuclein mutants by Lashuel et al.[10] Durell et al. have proposed a theoretical model for the channel structure of Aβ peptides.[11] In vivo, amyloid fibrils found in the brains of animals with scrapies resemble prion rods.[12] Large ribbonlike amyloid structures have been also observed for the $\alpha\beta$ peptide in the presence of Zn^{+2} ions.[7] Extensive research has been carried out on these different morphological structures, and several pathways have been postulated.[6,11,13] Nevertheless, a general mechanism covering these morphological structures possible in amyloid formation is still missing. An interesting question would be whether there is any correlation between these different morphological structures or if the structures are specific to a particular protein?

We hypothesized that the following two reasons could be responsible for the apparent lack (if any) of correlations between different morphologies. First, it is possible that many (if not all) morphological structures are present in other proteins as well; however, their transformation could be too slow to be followed by the experimental research. Second, it is possible that one of the particular structures is likely more stable, resulting in its predominant formation with the conversion rate from the unstable structures to the stable structure being too fast to detect intermediates. In this article, we used cytochrome c from *Saccharomyces cerevisiae* (cytc) and showed the formation of stable and rapid amyloids in the presence of SDS under mild experimental conditions (20 mM sodium phosphate buffer at pH 7.5 and at 25 °C). We chose this protein−surfactant pair because we expected that the binding between positively charged cytc and anionic surfactant SDS would provide a trigger in the form of partial unfolding to initiate the process of aggregation. The SDS-induced formation of the intermediate state of cytc has been studied before.[14,15] Salt-induced refolding of cytc has been shown to induce the aggregation of protein through domain swapping.[16] Local

Received: July 28, 2014
Revised: October 13, 2014

   dx.doi.org/10.1021/la5029993 | *Langmuir* XXXX, XXX, XXX−XXX

unfolding by the benzyl alcohol of cytc at and around Met 80 has been shown to induce aggregation.[17] It may also be noted that the interaction of SDS was shown to induce the formation of amyloid fibrils in α-synuclein.[18]

Although the role of cytc has not been directly implicated in any of the neurodegenerative diseases, amyloid formation of this protein has been reported.[19] More interestingly, the colocalization of α-synuclein and cytc has been observed in Lewy bodies of patients with Parkinson's disease.[20] It has been proposed that cytc may be involved in an "uncharacterized mechanism" that links apoptosis and neurodegeneration.[20] However, the interaction of cytc with phospholipids plays an important role in programmed cell death—apoptosis.[21] Under physiological conditions, cytc exists in equilibrium between a soluble native state and a membrane-bound conformation.[22] Free lipid molecules, which are not involved in the formation of the membrane, could interact with cytc. An interaction study of cytc with SDS (mimicking negatively charged phospholipids) with respect to apoptosis would also be interesting.

In this article, fluorescence correlation spectroscopy (FCS) has been used to study the interaction between cytc and SDS. FCS is an important single-molecule technique for studying diffusional and conformational properties of labeled biomolecules.[23] Using FCS in conjunction with other biophysical techniques, we have shown that cytc partially unfolds in the presence of SDS to form stable and rapid amyloid aggregates and the fraction of aggregated species correlates with the SDS concentration. In addition, we have captured many morphological structures of cytc aggregates using atomic force microscopy (AFM). These structures have appeared and disappeared in succession, with the final product being a huge mature rodlike structure. Although most of the structures have already been reported for different proteins, we have observed all of these structures formed by a single protein (cytc) and in the presence of a single experimental condition. In addition, we have observed an interesting porous honeycomb morphology, which could be involved as an intermediate.

EXPERIMENTAL SECTION

Materials. Iso-1-cytochrome c (C2436) and urea (CAS-13-6) were obtained from Sigma Chemical Company (St. Louis, MO). Sodium dodecyl sulfate (SDS, CAS no. 151-21-3) was purchased from USB. Tetramethyl rhodamine-5-maleimide (TMR) was obtained from Molecular Probes (Eugene, OR). All other reagents used were of the highest available grade. The cytc concentration was obtained by measuring the absorbance at 410 nm and using a molar extinction coefficient of 104 000 M^{-1} cm^{-1}.

CD Spectra. CD spectra were carried out using a Jasco J720 spectropolarimeter. Experiments were performed with 20 μM unlabeled proteins. Far-UV CD spectra were recorded over the 200−250 nm range, and each spectrum was averaged with 10 scans. For near-UV CD experiments (between 250 and 300 nm), almost 50 μM protein was used in a cuvette with a path length of 1 cm. Ten spectra were recorded in continuous mode and averaged.

Steady-State Fluorescence. The steady-state fluorescence experiments were carried out with unlabeled protein (not labeled with the extrinsic fluorophore) using a PTI fluorimeter (Photon Technology International, USA). The fluorescence emission spectra were recorded from 310 to 410 nm using an excitation wavelength of 295 nm, which eliminated emission from amino acids other than tryptophan. The final concentration of the cytc used for the steady-state fluorescence was 1 μM. Both CD and fluorescence experiments were carried out with 20 mM sodium phosphate buffer at pH 7.5.

For the THT binding experiments, the cytc and THT concentrations used were 1 and 10 μM, respectively. The samples were excited at 440 nm, and the emission spectra were recorded between 460 and 550 nm. For the Congo red binding experiments, the absorption spectra of cytc (2 μM) in the absence and presence of SDS were recorded between 450 and 650 nm using a Shimadzu 1700 Pharmaspec UV−vis spectrophotometer. Congo red (20 μM) was used for this study.

AFM Experiments. For AFM imaging, 10 μL of the samples was deposited on a freshly cleaved muscovite ruby mica sheet (ASTM V1 grade ruby mica from MICAFAB, Chennai) for 30 min. Mica sheets are negatively charged, so cytc (positively charged at pH 7.5) binds strongly to the mica surface. After 30 min, the sample is dried with a vacuum dryer. Sometimes the sample was gently washed with 0.5 mL of Milli-Q water to remove the molecules that were not firmly attached to the mica, and the sample was dried as mentioned above.

Acoustic alternate current (AAC) mode AFM was performed using a Pico Plus 5500 AFM (Agilent Technologies, USA) with a piezoscanner having a maximum range of 9 μm. Microfabricated silicon cantilevers of 225 μm in length with a nominal spring force constant of 21−98 N/m were obtained from Nano Sensors. The cantilever oscillation frequency was tuned to the resonance frequency. The cantilever resonance frequency was 150−300 kHz. The images (256 pixels × 256 pixels) were captured with a scan size of between 0.5 and 5 μm at a scan speed of 0.5 lines/s. Images were processed by flattening using PicoView software (Agilent Technologies, USA). All of the images presented in this report were derived from the original data. The length, height, and width of protein fibrils were measured manually using PicoView software.

FCS Experiments. FCS experiments were carried out using a commercial Confocor 3 LSM instrument (Carl Zeiss, Evotec, Jena, Germany) with a 40× water-immersion objective. Typically, 500 μL of the sample (labeled protein) was placed in Nunc chambers (NalgeNunc) and excited with an argon laser at 514 nm. The fluorescence signal was separated from the excited line using a main dichroic filter and collected using a pair of Avalanche photodiodes (APD). The photocurrent detected by the detectors was used to calculate the single-color cross-correlation function.

Labeling of cytc with TMR. A solution of TMR was slowly added to a 1 mg/mL solution of cytc with constant stirring. The molar ratio of the dye and the protein was kept at 1:1. The resulting solution was incubated for 6 h at 4 °C with shaking after every 30 min, and the excess free dye was removed by extensive dialysis followed by column chromatography using a Sephadex G25 column equilibrated with 20 mM sodium phosphate buffer at pH 7.5. The labeling of cytc with TMR does not significantly affect the structure, conformation, and folding of the protein (data not shown).[24] The extent of labeling was calculated to be approximately 50%.

Analysis of the Correlation Functions. For a system of one diffusing species without any conformational events, the diffusion time (τ_D) of the labeled species and average number of particles (N) present in the observation volume can be calculated by fitting the correlation function ($G(\tau)$) to eq 1.[25]

$$G(\tau) = 1 + \frac{1}{N}\frac{1}{\left(1+\frac{\tau}{\tau_D}\right)}\frac{1}{\left(1+S^2\frac{\tau}{\tau_D}\right)^{1/2}} \quad (1)$$

$G(\tau)$ corresponds to the correlation function of the diffusing species, and S is the structure parameter, the depth to diameter ratio of the Gaussian observation volume.

For a system of multidiffusing species, $G(\tau)$ can be represented by eq 2.[26]

$$G(\tau) = 1 + \frac{1}{N}\sum_i \frac{A_i}{1+\left(\frac{t}{\tau_{D_i}}\right)}\frac{1}{\left(1+S^2\left(\frac{t}{\tau_{D_i}}\right)\right)^{1/2}} \quad (2)$$

For the aggregating system, we considered the value of i to be 2. The first component (diffusion time τ_{D_1} and amplitude a_1) corresponds to the monomeric folded state of cytc, and the second component (diffusion time τ_{D_2} and amplitude a_2) corresponds to the cytc

dx.doi.org/10.1021/la5029993 | Langmuir XXXX, XXX, XXX−XXX

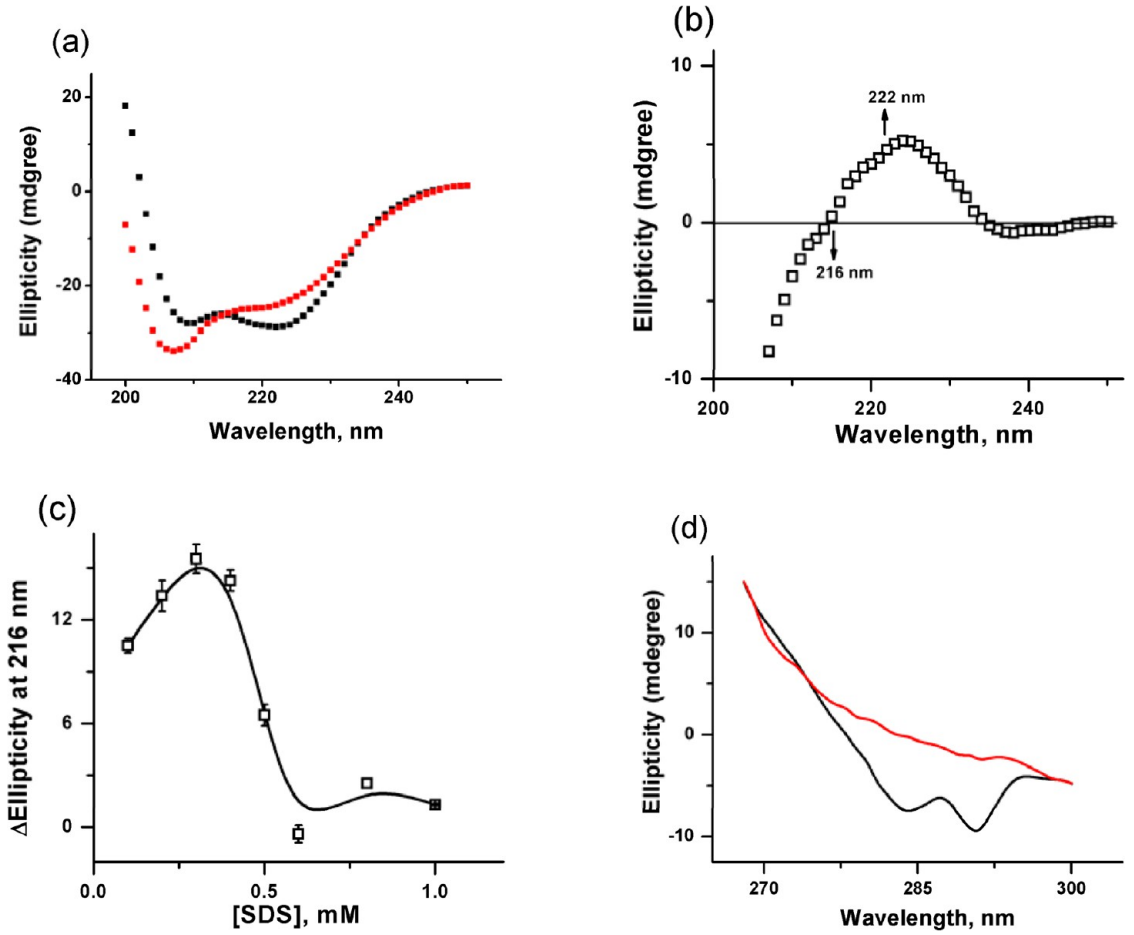

Figure 1. (a) Far-UV CD spectra of cytc in the absence (black) and presence of 1 mM SDS (red) and (b) the difference CD spectrum observed in the presence of 1 mM SDS. For this, the CD spectrum of cytc obtained in the absence of SDS has been used as a baseline. (c) Variation of elipticity at 216 nm (obtained from the difference spectra) with SDS concentration. (d) Near-UV CD spectra of cytc in the absence (black) and presence of 1 mM SDS (red). Experiments were carried out at 25 °C using 20 mM phosphate buffer at pH 7.5.

aggregates. It may be noted that the present model of two-component analysis is only a qualitative presentation of the complicated and heterogeneous process of aggregation that completely ignores the change in brightness due to aggregation.

The diffusion coefficient (D) of the protein molecules can be calculated from τ_D using eq 3

$$\tau_D = \frac{\omega^2}{4D} \tag{3}$$

where ω is the beam radius of the observation volume, which can be obtained by measuring the diffusion time of a dye with a known diffusion coefficient (D).

The hydrodynamic radius (r_H) of a labeled molecule can be calculated from D using eq 4 (Stokes–Einstein equation)

$$D = \frac{kT}{6\pi\eta r_H} \tag{4}$$

where k is the Boltzmann constant, η corresponds to the viscosity of the solution, and T is the temperature.

RESULTS AND DISCUSSION

Interaction between cytc and SDS Leads to a Significant Change in the Secondary and Tertiary Structure of the Protein. Structural and conformational changes of a protein as a result of its interaction with surfactants or lipid have been reported before.[14,27] The solvation dynamics of SDS-induced intermediates of cytc has been studied using femtosecond time-resolved fluorescence spectroscopy.[15] To monitor the structural and conformational changes of cytc in the presence of SDS, we have used CD as one of the preferred methods. The far-UV CD spectrum of the native folded protein is characterized by two minima at 208 and 222 nm (Figure 1a), which are characteristic of an α-helical protein. The interaction of cytc with 1 mM SDS leads to a small but significant change in the far-UV spectrum (Figure 1a). The difference CD spectrum calculated using the CD data obtained in the presence and absence of SDS (Figure 1b) shows a decrease in the 222 nm peak (indicating the depletion of the α-helix) and the appearance of a negative peak at 216 nm (suggesting the formation of the β-sheet). Figure 1c plots the variation of ellipticity at 216 nm obtained from the difference spectra with SDS concentration, which shows a cooperative increase in the β-sheet character. The conversion between an α-helix and a β-sheet intermediate has been shown in the case of α-synuclein.[28]

Near-UV CD (250–350 nm) was used to monitor the tertiary structure of cytc in the absence and presence of SDS, and the results are shown in Figure 1d. The interaction with SDS leads to a disruption of the tertiary structure of the protein. The near-UV CD spectrum of cytc in aqueous buffer shows minima at 282 and 288 nm, which correspond to the tertiary structural packing of the tryptophan residues as demonstrated before.[29] However, near-UV CD shows the complete disappearance of near-UV CD (Figure 1d),

dx.doi.org/10.1021/la5029993 | Langmuir XXXX, XXX, XXX–XXX

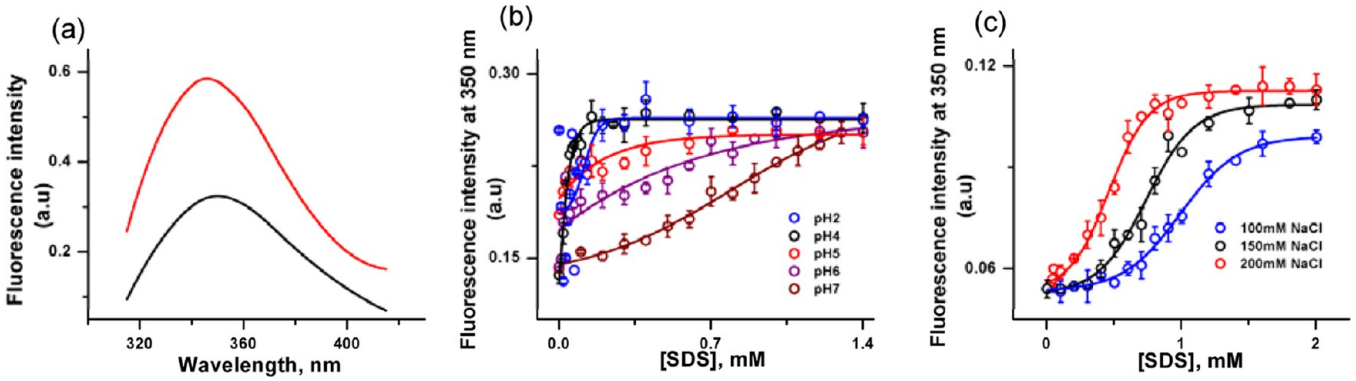

Figure 2. (a) Steady-state tryptophan fluorescence intensity of cytc in the absence (black) and presence of SDS (red). The variation in the tryptophan fluorescence intensity of cytc with SDS concentration at different pH values (b) and salt concentrations (c). The emission intensity at 350 nm was plotted, and the excitation wavelength used was 295 nm. Experimental conditions are the same as in Figure 1.

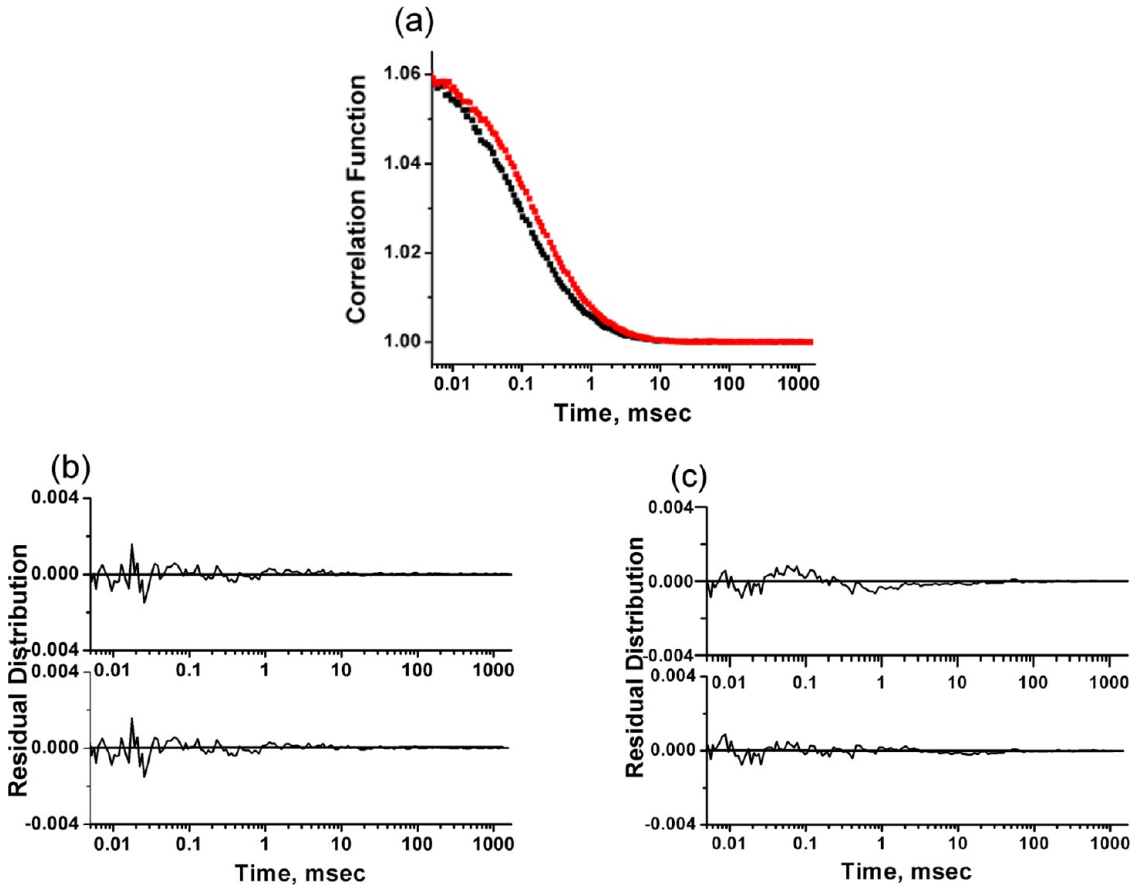

Figure 3. (a) Correlation functions obtained by FCS experiments using the cytc-TMR molecule in the absence and presence of 1 mM SDS (after 30 min of incubation). The use of eq 1 has been found to be appropriate to fit the autocorrelation function data obtained in the absence of SDS, which is evident by the randomness of the residual distribution (b, upper figure). The addition of an extra diffusional component does not improve the fit or the residual distribution (b, bottom figure). In the presence of 1 mM SDS, eq 1 yields nonrandom behavior of the residual distribution, suggesting that eq 1 may not be appropriate to fit the autocorrelation functions (c, upper figure). In contrast, this correlation function could be fit successfully to eq 2 (c, bottom figure).

suggesting the unfolding of the tertiary structure as a result of SDS interaction.

Steady-State Tryptophan Fluorescence Shows SDS-Induced Partial Unfolding. Tryptophan fluorescence is a convenient method of studying the local conformation of a protein around the tryptophan residue. cytc in its sequence has a single tryptophan residue, which yields quenched fluorescence emission (Figure 2a). The large quenching of tryptophan fluorescence emission intensity comes from the efficient energy transfer through the cofactor heme. The presence of 1 mM SDS leads to a large increase in the fluorescence intensity and a slight red shift of the emission maximum (Figure 2a). The interaction with SDS results in partial unfolding of the protein, leading to an increase in the distance between the tryptophan residue and heme.

dx.doi.org/10.1021/la5029993 | *Langmuir* XXXX, XXX, XXX–XXX

To understand the effect of SDS on the conformational change of cytc, tryptophan fluorescence, measured at 350 nm, has been used in the presence of different concentration of SDS at 25 °C (Figure 2b). In the tryptophan fluorescence measurement, protein solutions were excited at 295 nm and their emission spectra were recorded from 310 to 410 nm. Figure 2b plots the increase in the steady-state fluorescence intensity as a function of the concentration of SDS.

Although the critical micelle concentration (cmc) of SDS in water is 8 mM, its value can change in the presence of a protein. It has been shown in the case of other proteins that the surfactant forms small micellelike structures at an SDS concentration around or even less than 1 mM, and these small micelles can interact with the protein.[30] We have carried out a systematic pH and salt concentration dependence study to verify this model qualitatively. Both the decrease in pH and the increase in salt concentration have been shown to decrease the values of cmc for SDS.[31] The pH and salt concentration dependence data are shown in Figure 2b,c, respectively. The midpoint of the transitions corresponding to the SDS-induced partial unfolding decreases significantly as the pH of the solution decreases (Figure 2b). Identical results have been observed for the salt concentration dependence (Figure 2c).

FCS Suggests the Formation of Oligomeric Proteins in the Presence of SDS. FCS is an important technique for monitoring the diffusional and conformational dynamics of fluorescently labeled molecules at single-molecule resolution.[26,32,33] FCS, on the basis of the fluctuation analysis of the fluorescence with an observation volume on the order of a femtoliter containing a small number of molecules, provides quantitative information on the physical and chemical kinetics on the microsecond time scale. Intensity fluctuations may arise as a result of the (i) diffusion of the molecule with diffusion time τ_D in or out of the observation volume (eq 1) or (ii) the kinetics of a conformational change (with the time constant of τ_R) having a faster rate than the molecular diffusion ($\tau_R \ll \tau_D$).

For the FCS experiments, yeast cytc containing cysteine at position 102 was labeled with TMR. It was shown earlier that the TMR-labeled protein (cytc-TMR) shows an unaltered conformation and folding stability compared to that of the unlabeled protein.[24] Single color cross-correlation functions obtained with cytc-TMR in the absence and presence of 1 mM SDS are shown in Figure 3. In the absence of SDS, a model containing a diffusional component (eq 1 with a diffusion time of τ_D) has been used to fit the correlation data. It may be noted that the correlation function of the natively folded cytc needs an exponential component to account for its conformational fluctuations.[34] We have ignored the contribution of this component in most of the data analyses presented in this article. For this purpose, most of the data analyses are carried out by excluding up to 30 μs of the correlation data. We have observed identical values of τ_D with the correlation function starting from 10 μs using a single diffusion and exponential function and with the truncated correlation function (starting at 30 μs) using a single diffusion model.

FCS experiments in the presence of SDS showed a time dependence. An FCS measurement performed instantaneously after the addition of 1 mM SDS leads to a correlation function that typically can be fit using one diffusing component. The presence of a second component becomes apparent when the protein is incubated with time at 25 °C. All of the FCS experiments described here are carried out using an incubation time of 30 min, and we have used a two-component diffusion fit to analyze FCS data in the presence of SDS. The residual distributions of the fits using different models are also shown in Figure 3. The fast diffusion time (τ_{D_1}) corresponds to the monomeric protein, which is similar to the diffusion time obtained in the absence of SDS. The relatively slow component (with a diffusion time of τ_{D_2}) represents the oligomers, the formation of which has been induced by the presence of SDS. Figure 4 shows the variation of the amplitudes of the first

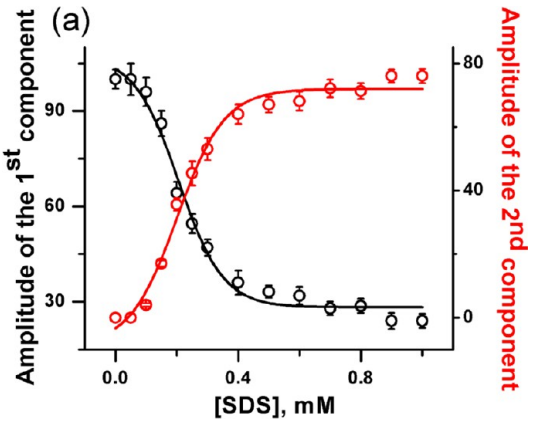

Figure 4. Amplitudes of the first (monomeric protein) and second (oligomers) components obtained from the FCS experiments are plotted against SDS concentration. All of these data have been obtained after 30 min of incubation.

(monomeric protein) and second (oligomers) components obtained from the FCS experiments in the presence of different SDS concentrations. The fraction of the monomeric component (with a diffusion time of τ_{D_1}) decreases, which is accompanied by a simultaneous increase in the fractions of the oligomeric species (with a diffusion time of τ_{D_2}).

Using eq 3 and 4, we have calculated the hydrodynamic radii (r_H) of the monomeric and aggregated cytc from the values of τ_D. In the absence of SDS, the value of r_H has been observed to be 22 Å. This value matches the early reports[35] and corresponds very well to the expected value of r_H for a globular protein of similar molecular weight.[36] In the presence of 1 mM SDS, the value of r_H for the slow component increases to 132 Å. This value of r_H is significantly larger than the value of r_H for the completely unfolded cytc obtained in the presence of 10 M urea (40 Å).[35] This is expected because of the formation of the high-molecular-weight oligomers of cytc. Although it is difficult to characterize the oligomers using the present data, it may be mentioned that the observed r_H is much larger than the r_H of SDS micelles (about 22 Å), which has been determined by FCS experiments with 10 mM SDS.[31] It may also be noted that the value of r_H is considerably larger than that observed in the presence of a ionic liquid.[37]

The protein samples in the presence of 1 mM SDS have been incubated at 25 °C for a longer time, and FCS experiments have been carried out at different time points to find out if there is any further change. The correlation functions obtained at different time points are shown in Figure 1Sa (Supporting Information). As described above, FCS data taken immediately after the addition of SDS do not require a second component, and the calculated r_H is similar to the value reported earlier.[37] It may be noted that a long incubation time results in significantly complex correlation functions. The tail effect present in the

dx.doi.org/10.1021/la5029993 | Langmuir XXXX, XXX, XXX–XXX

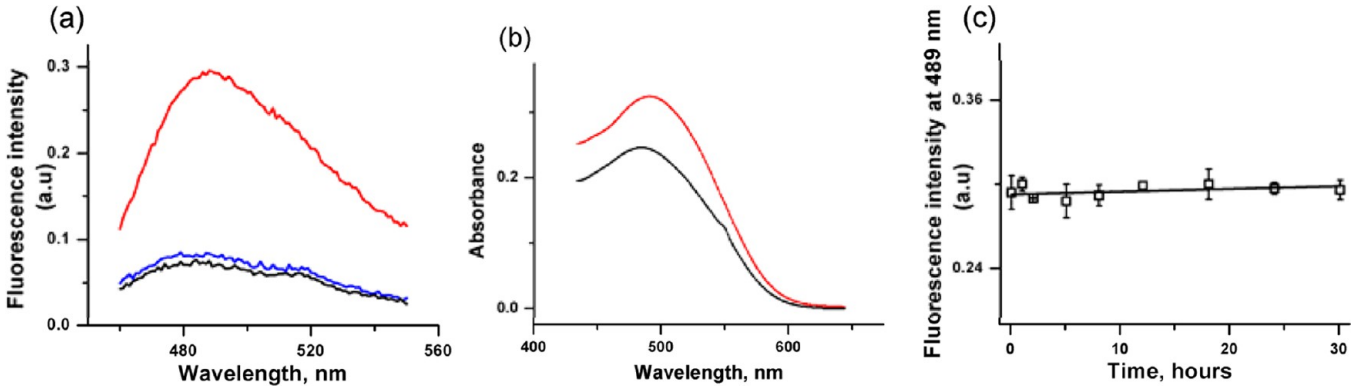

Figure 5. (a) Fluorescence emission spectra of THT (blue line) and cytc in the absence (black line) and presence of 1 mM SDS (red line), (b) Congo red absorption spectra of cytc in the absence (black line) and presence of 1 mM SDS (red line), and (c) variation of THT intensity of cytc + 1 mM SDS with time. The fluorescence intensity remained constant for 24 h. Experimental conditions are the same as in Figure 1.

correlation functions observed in the case of long incubation time (6 and 30 h of data as shown in Figure 1Sa, Supporting Information) makes even a two-component diffusion model inappropriate to fit these data (residual distribution shown in Figure 1Sb, Supporting Information). Additionally, the intensity fluctuation data during the long-time incubation results in large spikes (Figure 1Sc, Supporting Information). The presence of large spikes and the associated tail effect in the correlation function have been observed in the case of the oligomerization of the intestinal fatty acid binding proteins.[26] The value of r_H corresponding to the slow component increases with the time of incubation (Figure 1Sd, Supporting Information).

SDS-Induced Oligomers Show Amyloid-like Character. As discussed, the interaction of cytc with SDS results in the partial unfolding of the protein, forming a β-sheet-like structure. FCS studies suggested that the SDS-induced partial unfolding results in the formation of oligomeric species. To obtain further insight into the nature of the oligomers, we used thioflavin T (THT) fluorescence and Congo red binding measurements. These two methods (THT fluorescence and Congo red binding assays) are routinely used to study the amyloid behavior of a protein. THT is a benzothiazole dye that exhibits enhanced fluorescence emissions upon binding to amyloid fibrils but does not bind to amorphous aggregates.

When native cytc in aqueous buffer was incubated with THT, no fluorescence was observed, but in the presence of 1 mM SDS, a large increase in THT fluorescence emission spectra was found (Figure 5a). All of the THT binding experiments reported here are carried out after incubating the protein samples for 30 min in the presence of SDS. Because THT has a background fluorescence signal in the presence of SDS, the data shown in Figure 5a have been corrected using identical-concentration SDS as a background. Similarly, Figure 5b shows an increase in the Congo red absorption spectra of cytc in the absence and presence of 1 mM SDS. Increases in THT fluorescence and Congo red absorption indicate the formation of amyloid fibrils in the presence of 1 mM SDS. It is to be noted that no increase in the THT fluorescence intensity was observed when cytc was added to a THT solution in the absence of SDS, suggesting the importance of SDS in the process of amyloid formation. THT fluorescence observed with cytc in the presence of 1 mM SDS remained constant for 24 h, suggesting that the aggregates are amyloid-like in nature (Figure 5c).

SDS-Induced Aggregates of cytc Change Their Morphologies with Time. We have shown that cytc unfolds partially in the presence of 1 mM SDS, and this intermediate contains β-sheet-like character. We have observed a rapid increase in THT fluorescence, which is significantly faster than that for α-synuclein, which needs multiple days for amyloid formation under in vitro conditions.[18] This faster kinetics allows us to monitor subsequent slower events, and FCS data show time-dependent oligomerization. Because it is difficult to model the FCS data for an accurate estimation of the oligomer size and there have been additional problems of complicated correlation functions observed at slow time points, we have used AFM as the method of choice for further characterization of the time dependence. AFM is a common technique for the direct visualization of protein aggregates, without requiring any staining protocol. The protein solution (1 μM) in the presence of different SDS concentrations was subsequently incubated at 25 °C and analyzed at different time intervals using AFM.

After 3 h of incubating cytc with 1 mM SDS, the presence of thin fibrils of cytc is observed. These fibrils have a width of 10 nm (Figure 6a). An increase in THT fluorescence shows that these are amyloid fibrils (Figure 5a). Thin fibrils with almost the same morphology have been observed previously for α-synuclein and $\alpha\beta$ peptide.[38,39] With time, these thin fibrils have been found to stick together to form large sheetlike structures with a width of 3200 nm (Figure 6c). A closer look into these sheetlike structure shows that they are formed by multistranded thin fibrils (width of 10 nm) that are laterally associated with each other (bottom of Figure 6c). Similar multistranded fibrils have been observed for lysozyme and β lactoglobulin at high temperature and acidic pH by Lara et al. After 6 h of incubation, differently sized pores are found to form in the sheetlike structure (Figure 6d). We have found an increase in the pore size with time.

After 7.5 h, the pores are found to become sufficiently large with the fibrils assembled into a hexagonal morphology looking like honeycombs (Figure 7a). In the honeycomb-like structure, the fibrils arrange themselves in close-packed arrays of ordered hexagonal cells each containing a central pore. The height of the pore is 4 nm, and the pore has been found to extend up to the mica surface (bottom of Figure 7). Similar pore formation of PerfringolysinO was observed by Lashuel et al.[10] The width of the filaments in the honeycomb-like structure has been found to vary from 50 to 120 nm. In contrast, the pore size is varied from 200 to 400 nm. A close investigation of the filament

dx.doi.org/10.1021/la5029993 | Langmuir XXXX, XXX, XXX−XXX

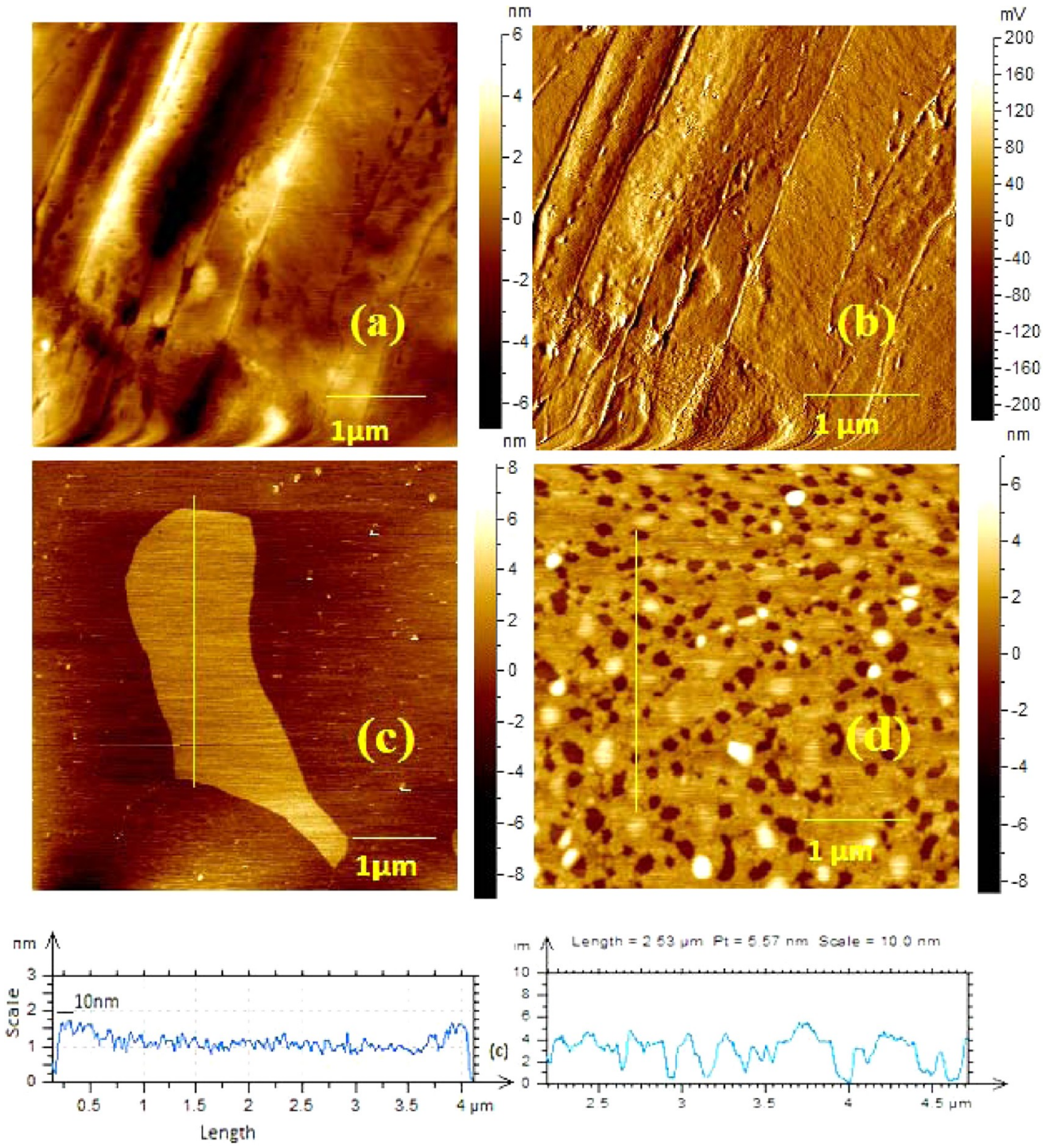

Figure 6. AFM images of cytc after incubating for (a) 3 h, (b) 3 h (amplitude image), (c) 5 h, and (d) 6 h in the presence of 1 mM SDS. After 3 h of incubating cytc in SDS, we observed thin fibrils (a). For better resolution, amplitude image (b) was also provided with topography image (a). The thin fibrils stuck together to form a sheetlike structure (c). The bottom of Figure 1c shows that the sheetlike structure consisted of several thin fibrils. After 5 h, pores of different size were observed (d). Experiments were carried out at room temperature using 20 mM phosphate buffer at pH 7.5.

structure show that the width of the individual building block of the thin fibrils in the honeycomb-like state is around 10 nm, which has indicated that this honeycomb-like structure may be the later stage of thin and sheet-like fibrils observed initially. With time, the pore diameters in the honeycomb-like structure have been found to increase, and a significant increase occurs after 1 day compared to the observed diameter after 7.5 h (Figure 7b). Figure 7 shows the difference in the honeycomb-like structures formed after 7.5 h and that after 1 day. To investigate if the variations in sample preparations have any role in the morphology, the initial samples have been prepared using different methods by using glass and Eppendorf tubes and by changing the order of cytc and SDS addition. We have not observed any significant variations in the morphologies, and these structures do not depend on sample preparation. In addition, their formation has been reproduced using different

dx.doi.org/10.1021/la5029993 | *Langmuir* XXXX, XXX, XXX–XXX

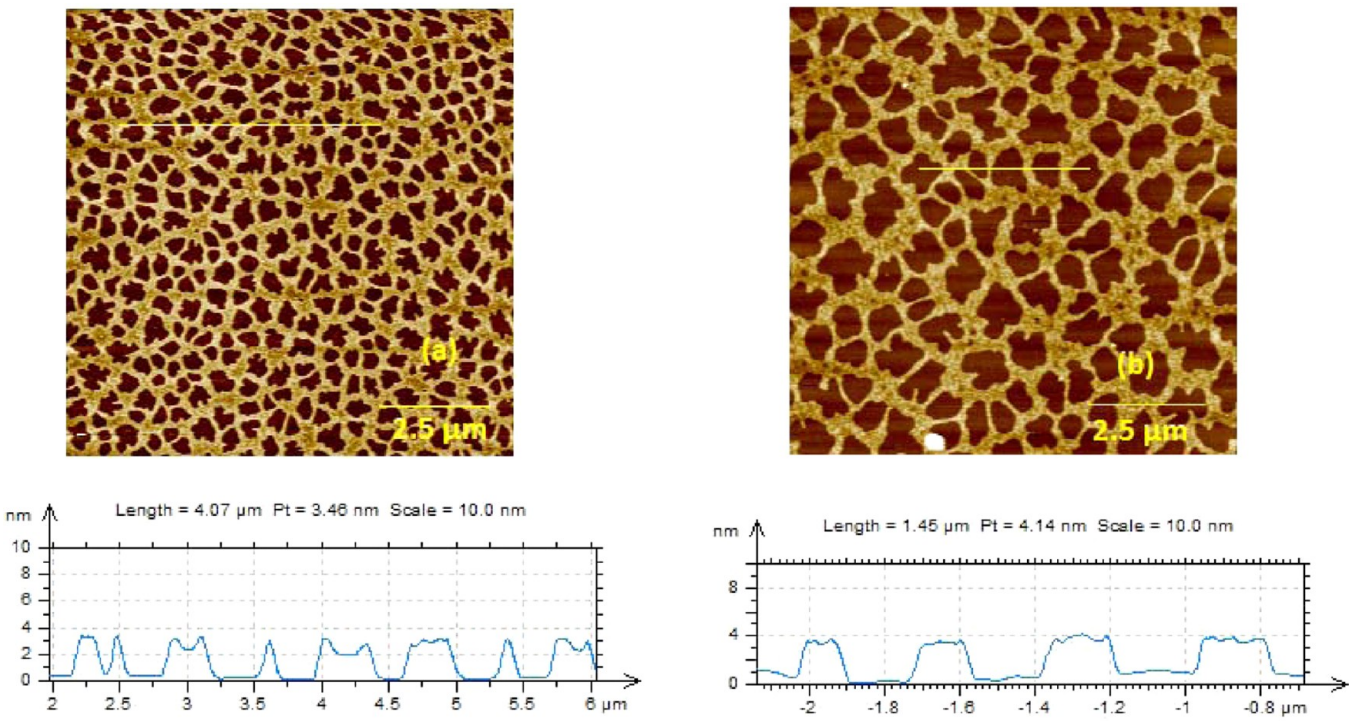

Figure 7. Honeycomb-like structure observed with cytc after incubating for (a) 7.5 h and (b) 1 day in the presence of 1 mM SDS. The pores of the honeycomb-like structure observed after 1 day were much larger than that observed after 7.5 h. Both images have been taken using the same scale.

sample volumes, which rule out the possibility of artifacts arising from air drying.

After 2 days, these honeycomb-like structures are found to be disrupted, with the aggregated proteins concentrated on one side of the mica sheet (Figure 8a). After 3 days, the aggregated proteins dissociate completely to form small globular oligomers (Figure 8b). It has been observed with time that the oligomeric aggregates have started rearranging themselves in collinear fashions (4 days, Figure 8c). The formation of linear fibrils, which connect these oligomers, has been found to occur (Figure 8d). A closer look reveals that the oligomers, which are attached to the fibril, are not spherical but rather oval in shape, whereas those that are not attached to the fibril remain spherical (6 days, Figure 8e). After 15 days, a highly twisted rod-shaped structure is observed with a well-defined average height of 11 nm and a typical width in the range of 70 to 90 nm (Figure 8f). Long homogeneous ribbonlike amyloid structures of a similar kind have been reported by Lynn and coworkers.[7] Rodlike amyloids have been observed for prion proteins, synthetic polypeptides [poly(ValGlyGlyLeuGly)], and human serum transferrin as well.[12,40]

Our initial assumption has been that the increase in speed in amyloid formation may enable us to observe different morphologies. This assumption has been supported by a temperature-dependence study in which the above experiments have been carried out at elevated (90 °C) as well as lower temperature (4 °C). The mature rodlike fibrils that have been observed after 15 days at 25 °C are formed overnight when cytc is incubated at 90 °C (Figure 2S, Supporting Information). In contrast, no fibril has been observed even after 25 days of incubation at 4 °C (data not shown).

Furthermore, we have studied the protein and SDS concentration dependence using steady-state fluorescence and AFM. For the protein-concentration-dependence experiments, two concentrations of 1 and 5 μM have been used. Figure 3S (Supporting Information) shows the variation in steady-state fluorescence intensity with SDS concentration. Both these data and the results obtained from AFM experiments (data not shown) do not show any apparent protein-concentration dependence, at least in the range between 1 and 5 μM. Figure 4S (Supporting Information) shows AFM images obtained with 1 μM protein in the presence of 250 and 750 μM SDS with incubation times of 3 and 10 h. No significant population of aggregates of any morphology has been observed with 250 μM SDS at 3 h. However, oligomeric aggregates with size ranging between 20 and 100 nm have started appearing with 250 μM SDS after 10 h of incubation (Figure 4S, Supporting Information). A similar result has also been observed with 500 μM SDS (not shown). In contrast, the conversion between different morphologies has been found to occur with 750 μM SDS, suggesting a critical role of the SDS concentration in this process. It may be noted that the oligomerization of cytc is not observed in the absence of SDS (Figure 5S, Supporting Information).

The mechanism of cytc oligomerization and aggregation is not well understood. It has been shown that the polymerization of this protein occurs through successive domain swapping.[41] The crystal structures of dimeric and trimeric cytc are also available, and these results strongly suggest that the polymerization process retains the α-helical structure.[42] In contrast, FTIR studies have suggested that the precipitate of cytc induced by an intermediate concentration of SDS contains an intermolecular β-sheet configuration.[43] Another study carried out in a mild alkaline environment has suggested that the amyloid formation of cytc requires the presence of an unfolded state region.[44] All of these results in combination with the data shown here strongly emphasize the heterogeneity of the aggregation pathways and the importance of using complementary techniques, preferably those with single-molecule sensitivity for aggregation studies.

dx.doi.org/10.1021/la5029993 | *Langmuir* XXXX, XXX, XXX−XXX

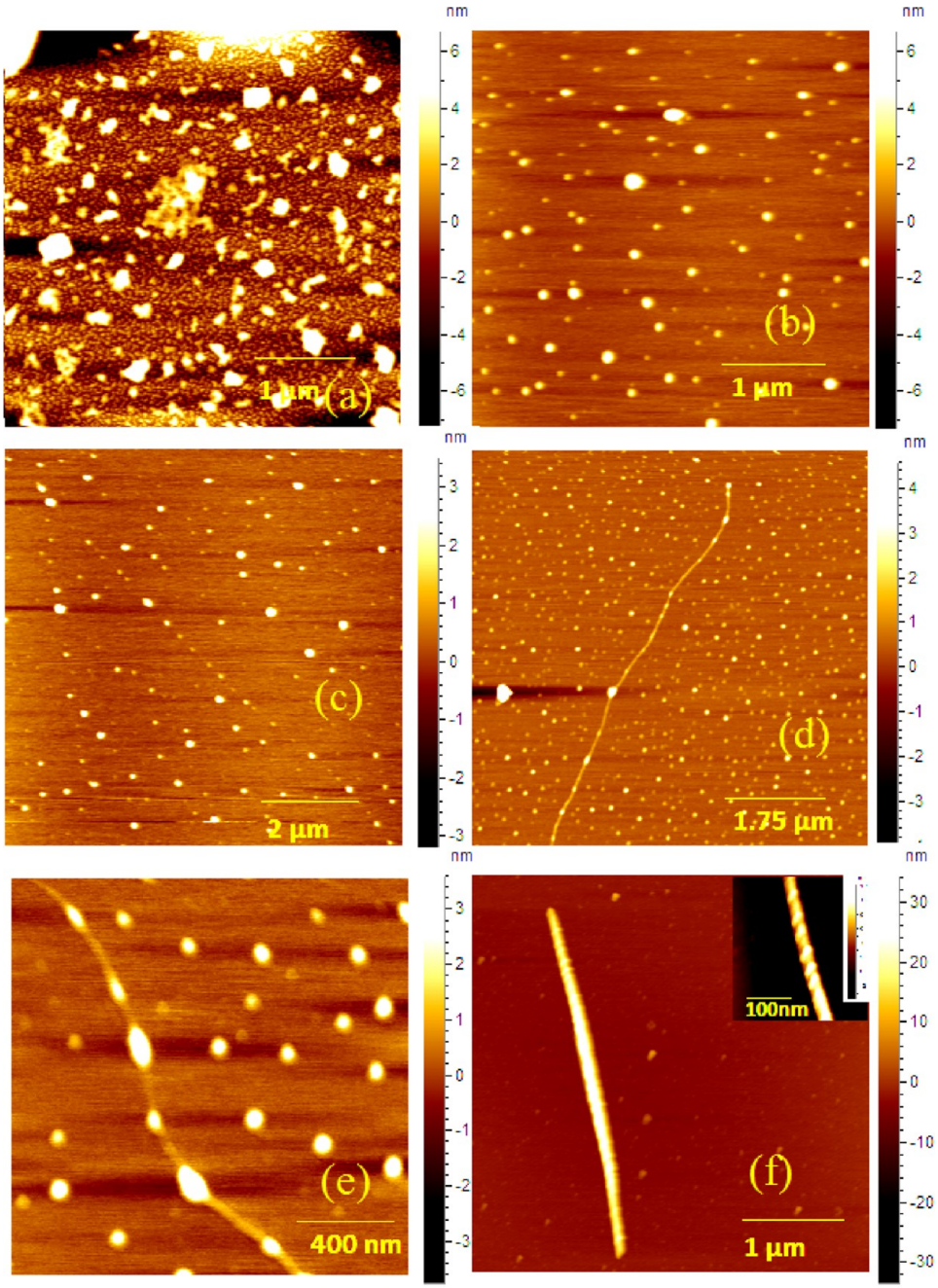

Figure 8. AFM images of cytc after incubating for (a) 2, (b) 3, (c) 4, (d) 5, (e) 6, and (f) 15 days in the presence of 1 mM SDS. After 2 days, the honeycomb-like structure started to be disrupted, with the aggregated protein concentrated on one side of the mica sheet (a). After 3 days, the aggregated proteins were found to be dissociated into spherical oligomers (b). On day 4, the spherical oligomers rearranged themselves in a linear fashion (c), after 5 days, thin fibrils were observed to connect the spherical oligomers (d), on day 6, the spherical oligomers became oval in shape and the attaching fibrils became thicker (e), and after 15 days, rodlike highly twisted matured fibrils were observed (f).

Various morphological structures of different proteins have been reported by multiple groups, and they have proposed different specific pathways to describe the formation of each individual morphological structure. However, biophysical experiments (such as Congo red birefringence and the THT staining assay) revealed that all of the different morphologies have similar properties, indicating possible interconnection between these structures. In our study, we have observed many of these previously reported structures in a single protein using AFM, and the combined data presented here suggest the possibility of a mechanism (sequential or otherwise) connecting these morphologies. We believe that these morphological structures could be present in other protein systems as well. The correlation of these structurally different amyloid fibrils on the molecular level may provide important clues to further our understanding of amyloid formation.

The uniqueness of the honeycomb-like and rod-shaped nanostructures may generate novel applications in nanotechnology. It can be mentioned that the structure of porous alumina templates has been represented as a closely packed honeycomb structure of hexagonal cores, each containing a pore at the center. Nanorods or nanowires can be synthesized

dx.doi.org/10.1021/la5029993 | *Langmuir* XXXX, XXX, XXX−XXX

inside the pores of these templates by controlling the anodization time and voltage.[45] The honeycomb-like nanostructures observed in the present study may be used as a biotemplate for the formation of softer nanotubes or nanowires. The rod-shaped hollow nanostructures have been shown to have a range of applications in the design of nanobiomaterials or for drug-delivery devices. It is important to note that the rod-shaped nanostructures observed by us are also stable at high temperatures (experiments carried out at 90 °C, Figure 2S). It is also important to note that these structures are formed at room temperature under physiological buffer conditions, without requiring high temperature or difficult experimental setups. To discover more potential applications of rodlike or honeycomb-like amyloid fibrils, physical experiments with these structures are carried out in our laboratory.

CONCLUSIONS

We show that cytc is partially unfolded in the presence of a premicellar concentration of SDS to form oligomeric structures. These structures bind THT and Congo red and interconvert between different morphologies. To the best of our knowledge, this is the first report of the presence of different morphologies of amyloid fibrils in a single heme protein (cytc). The correlation of these structurally different amyloid fibrils in a single protein on the molecular level may provide important clues to further our understanding of amyloid formation. An interesting honeycomb-like intermediate was also identified in this process. We believe that the uniqueness of the honeycomb-like and rodlike structures (that have been identified in this process) might have the potential to be used as a template for nanobiotechnological applications.

ASSOCIATED CONTENT

Supporting Information

Variation of the correlation functions of cytc-TMR with time in the presence of SDS. Rodlike amyloid fibril of cytc observed after overnight incubation in the presence of 1 mM SDS at 90 °C. Variation in the tryptophan fluorescence intensity with SDS at different cytc concentrations. AFM mages of cytc in presence of SDS after 3 h of incubation. AFM image taken after cytc was incubated for 6 days without SDS. This material is available free of charge via the Internet at http://pubs.acs.org/.

AUTHOR INFORMATION

Corresponding Author

*E-mail: krish@iicb.res.in. Tel: 011913324995843

Present Address

(S.H.) Max Planck Institute of Biochemistry, Department of Cellular Biochemistry, Am Klopferspitz 18, 82152 Martinsried, Germany.

Author Contributions

S.H. and P.S. made equal contributions to this work.

Notes

The authors declare no competing financial interest.

ACKNOWLEDGMENTS

This study has been funded by CSIR network project grant UNSEEN. K.C. acknowledges the Director, CSIR-IICB for the help and encouragement. S.H. thanks Amit J. Gupta and Jayati Sengupta for their critical comments on the manuscript.

REFERENCES

(1) Hamada, D.; Yanagihara, I.; Tsumoto, K. Engineering amyloidogenicity towards the development of nanofibrillar materials. *Trends Biotechnol.* **2004**, *22*, 93−97.
(2) Selkoe, D. J. Folding proteins in fatal ways. *Nature* **2003**, *426*, 900−904.
(3) Eichner, T.; Radford, S. E. A diversity of assembly mechanisms of a generic amyloid fold. *Mol. Cell* **2011**, *43*, 8−18.
(4) Chiti, F.; Dobson, C. M. Protein misfolding, functional amyloid, and human disease. *Annu. Rev. Biochem.* **2006**, *75*, 333−366.
(5) Eisenberg, D.; Jucker, M. The amyloid state of proteins in human diseases. *Cell* **2012**, *148*, 1188−1203.
(6) Lara, C.; Adamcik, J.; Jordens, S.; Mezzenga, R. General self-assembly mechanism converting hydrolyzed globular proteins into giant multistranded amyloid ribbons. *Biomacromolecules* **2011**, *12*, 1868−1875.
(7) Dong, J.; Shokes, J. E.; Scott, R. A.; Lynn, D. G. Modulating amyloid self-assembly and fibril morphology with Zn(II). *J. Am. Chem. Soc.* **2006**, *128*, 3540−3542.
(8) Fauerbach, J. A.; Yushchenko, D. A.; Shahmoradian, S. H.; Chiu, W.; Jovin, T. M.; Jares-Erijman, E. A., Supramolecular non-amyloid intermediates in the early stages of alpha-synuclein aggregation. *Biophys. J.* **2012**, *102*, 1127−1136.
(9) Nicoll, A. J.; Panico, S.; Freir, D. B.; Wright, D.; Terry, C.; Risse, E.; Herron, C. E.; O'Malley, T.; Wadsworth, J. D.; Farrow, M. A.; Walsh, D. M.; Saibil, H. R.; Collinge, J. Amyloid-beta nanotubes are associated with prion protein-dependent synaptotoxicity. *Nat. Commun.* **2013**, *4*, 2416.
(10) Lashuel, H. A.; Hartley, D.; Petre, B. M.; Walz, T.; Lansbury, P. T., Jr. Neurodegenerative disease: amyloid pores from pathogenic mutations. *Nature* **2002**, *418*, 291.
(11) Atamna, H.; Boyle, K. Amyloid-beta peptide binds with heme to form a peroxidase: relationship to the cytopathologies of Alzheimer's disease. *Proc. Natl. Acad. Sci. U.S.A.* **2006**, *103*, 3381−3386.
(12) McKinley, M. P.; Meyer, R. K.; Kenaga, L.; Rahbar, F.; Cotter, R.; Serban, A.; Prusiner, S. B. Scrapie prion rod formation in vitro requires both detergent extraction and limited proteolysis. *J. Virol* **1991**, *65*, 1340−1351.
(13) Alakoskela, J. M.; Jutila, A.; Simonsen, A. C.; Pirneskoski, J.; Pyhajoki, S.; Turunen, R.; Marttila, S.; Mouritsen, O. G.; Goormaghtigh, E.; Kinnunen, P. K. Characteristics of fibers formed by cytochrome c and induced by anionic phospholipids. *Biochemistry* **2006**, *45*, 13447−13453.
(14) Chattopadhyay, K.; Mazumdar, S. Stabilization of partially folded states of cytochrome c in aqueous surfactant: effects of ionic and hydrophobic interactions. *Biochemistry* **2003**, *42*, 14606−14613.
(15) Sahu, K.; Mondal, S. K.; Ghosh, S.; Roy, D.; Sen, P.; Bhattacharyya, K. Femtosecond study of partially folded states of cytochrome C by solvation dynamics. *J. Phys. Chem. B* **2006**, *110*, 1056−1062.
(16) Deshpande, M. S.; Parui, P. P.; Kamikubo, H.; Yamanaka, M.; Nagao, S.; Komori, H.; Kataoka, M.; Higuchi, Y.; Hirota, S. Formation of domain-swapped oligomer of cytochrome C from its molten globule state oligomer. *Biochemistry* **2014**, *53*, 4696−4703.
(17) Singh, S. M.; Cabello-Villegas, J.; Hutchings, R. L.; Mallela, K. M. Role of partial protein unfolding in alcohol-induced protein aggregation. *Proteins* **2010**, *78*, 2625−2637.
(18) Ahmad, M. F.; Ramakrishna, T.; Raman, B.; Rao Ch, M. Fibrillogenic and non-fibrillogenic ensembles of SDS-bound human alpha-synuclein. *J. Mol. Biol.* **2006**, *364*, 1061−1072.
(19) Pertinhez, T. A.; Bouchard, M.; Tomlinson, E. J.; Wain, R.; Ferguson, S. J.; Dobson, C. M.; Smith, L. J. Amyloid fibril formation by a helical cytochrome. *FEBS Lett.* **2001**, *495*, 184−186.
(20) Hashimoto, M.; Takeda, A.; Hsu, L. J.; Takenouchi, T.; Masliah, E. Role of cytochrome c as a stimulator of alpha-synuclein aggregation in Lewy body disease. *J. Biol. Chem.* **1999**, *274*, 28849−28852.
(21) Belikova, N. A.; Jiang, J.; Tyurina, Y. Y.; Zhao, Q.; Epperly, M. W.; Greenberger, J.; Kagan, V. E. Cardiolipin-specific peroxidase

reactions of cytochrome C in mitochondria during irradiation-induced apoptosis. *Int. J. Radiat Oncol Biol. Phys.* **2007**, *69*, 176−186.
(22) Cortese, J. D.; Voglino, A. L.; Hackenbrock, C. R. Multiple conformations of physiological membrane-bound cytochrome c. *Biochemistry* **1998**, *37*, 6402−6409.
(23) Chattopadhyay, K.; Elson, E. L.; Frieden, C. The kinetics of conformational fluctuations in an unfolded protein measured by fluorescence methods. *Proc. Natl. Acad. Sci. U.S.A.* **2005**, *102*, 2385−2389.
(24) Perroud, T. D.; Bokoch, M. P.; Zare, R. N. Cytochrome c conformations resolved by the photon counting histogram: watching the alkaline transition with single-molecule sensitivity. *Proc. Natl. Acad. Sci. U.S.A.* **2005**, *102*, 17570−17575.
(25) Hess, S. T.; Huang, S.; Heikal, A. A.; Webb, W. W. Biological and chemical applications of fluorescence correlation spectroscopy: a review. *Biochemistry* **2002**, *41*, 697−705.
(26) Sarkar, S.; Chattopadhyay, K. Studies of early events of folding of a predominately beta-sheet protein using fluorescence correlation spectroscopy and other biophysical methods. *Biochemistry* **2014**, *53*, 1393−1402.
(27) Pinheiro, T. J. The interaction of horse heart cytochrome c with phospholipid bilayers. Structural and dynamic effects. *Biochimie* **1994**, *76*, 489−500.
(28) Comellas, G.; Lemkau, L. R.; Zhou, D. H.; George, J. M.; Rienstra, C. M. Structural intermediates during alpha-synuclein fibrillogenesis on phospholipid vesicles. *J. Am. Chem. Soc.* **2012**, *134*, 5090−5099.
(29) Davies, A. M.; Guillemette, J. G.; Smith, M.; Greenwood, C.; Thurgood, A. G.; Mauk, A. G.; Moore, G. R. Redesign of the interior hydrophilic region of mitochondrial cytochrome c by site-directed mutagenesis. *Biochemistry* **1993**, *32*, 5431−5435.
(30) Giehm, L.; Oliveira, C. L.; Christiansen, G.; Pedersen, J. S.; Otzen, D. E. SDS-induced fibrillation of alpha-synuclein: an alternative fibrillation pathway. *J. Mol. Biol.* **2010**, *401*, 115−133.
(31) Haldar, S.; Chattopadhyay, K. Effects of arginine and other solution additives on the self-association of different surfactants: an investigation at single-molecule resolution. *Langmuir* **2011**, *27*, 5842−5849.
(32) Basak, S.; Chattopadhyay, K. Studies of protein folding and dynamics using single molecule fluorescence spectroscopy. *Phys. Chem. Chem. Phys.* **2014**, *16*, 11139−11149.
(33) Basak, S.; Chattopadhyay, K. Fluorescence correlation spectroscopy study on the effects of the shape and size of a protein on its diffusion inside a crowded environment. *Langmuir* **2013**, *29*, 14709−14717.
(34) Haldar, S.; Chattopadhyay, K. Interconnection of salt-induced hydrophobic compaction and secondary structure formation depends on solution conditions: revisiting early events of protein folding at single molecule resolution. *J. Biol. Chem.* **2012**, *287*, 11546−11555.
(35) Haldar, S.; Mitra, S.; Chattopadhyay, K. Role of protein stabilizers on the conformation of the unfolded state of cytochrome c and its early folding kinetics: investigation at single molecular resolution. *J. Biol. Chem.* **2010**, *285*, 25314−25323.
(36) Wilkins, D. K.; Grimshaw, S. B.; Receveur, V.; Dobson, C. M.; Jones, J. A.; Smith, L. J. Hydrodynamic radii of native and denatured proteins measured by pulse field gradient NMR techniques. *Biochemistry* **1999**, *38*, 16424−16431.
(37) Sen Mojumdar, S.; Chowdhury, R.; Chattoraj, S.; Bhattacharyya, K., Role of ionic liquid on the conformational dynamics in the native, molten globule, and unfolded states of cytochrome c: a fluorescence correlation spectroscopy study. *J. Phys. Chem. B* **2012**, *116*, 12189−12198.
(38) Yagi, H.; Ban, T.; Morigaki, K.; Naiki, H.; Goto, Y. Visualization and classification of amyloid beta supramolecular assemblies. *Biochemistry* **2007**, *46*, 15009−15017.
(39) Del Mar, C.; Greenbaum, E. A.; Mayne, L.; Englander, S. W.; Woods, V. L., Jr. Structure and properties of alpha-synuclein and other amyloids determined at the amino acid level. *Proc. Natl. Acad. Sci. U.S.A.* **2005**, *102*, 15477−15482.
(40) Ghosh, S.; Mukherjee, A.; Sadler, P. J.; Verma, S. Periodic iron nanomineralization in human serum transferrin fibrils. *Angew. Chem., Int. Ed. Engl.* **2008**, *47*, 2217−2221.
(41) Hirota, S.; Ueda, M.; Hayashi, Y.; Nagao, S.; Kamikubo, H.; Kataoka, M. Maintenance of the secondary structure of horse cytochrome c during the conversion process of monomers to oligomers by addition of ethanol. *J. Biochem.* **2012**, *152*, 521−529.
(42) Hirota, S.; Hattori, Y.; Nagao, S.; Taketa, M.; Komori, H.; Kamikubo, H.; Wang, Z.; Takahashi, I.; Negi, S.; Sugiura, Y.; Kataoka, M.; Higuchi, Y. Cytochrome c polymerization by successive domain swapping at the C-terminal helix. *Proc. Natl. Acad. Sci. U.S.A.* **2010**, *107*, 12854−12859.
(43) Xu, Q.; Keiderling, T. A. Effect of sodium dodecyl sulfate on folding and thermal stability of acid-denatured cytochrome c: a spectroscopic approach. *Protein Sci.* **2004**, *13*, 2949−2959.
(44) de Groot, N. S.; Ventura, S. Amyloid fibril formation by bovine cytochrome c. *Spectroscopy* **2005**, *19*, 199−205.
(45) Zhang, J.; Kielbasa, J. E.; Carroll, D. L. Controllable fabrication of porous alumina templates for nanostructures synthesis. *Mater. Chem. Phys.* **2010**, *122*, 295−300.